

Controllable half-vortex lattices in an incoherently pumped polariton condensate

Jonathan Keeling¹ and Natalia G. Berloff²

¹*SUPA, School of Physics and Astronomy, University of St Andrews, KY16 9SS, UK*

²*Department of Applied Mathematics and Theoretical Physics, University of Cambridge, CB3 0WA, UK*

(Dated: January 13, 2013)

We show how the transition between synchronized and desynchronized states of a spinor polariton condensate can be used to drive a transition between stationary vortex lattices and half-vortex lattices. This provides a way to control polariton spin textures by a combination of pump spot profile and applied magnetic fields. To do this, we extend the model of non-equilibrium spinor condensates to include relaxation, and study how this affects the desynchronization transition. We discuss how the pattern formation can be explained by behavior of the homogeneous system.

PACS numbers: 03.75.Kk, 47.37.+q, 71.36.+c, 71.35.Lk

Among the various topological defects that may exist in superfluids and superconductors, quantized vortices receive particular theoretical and experimental attention. These localized nonlinear structures are nontrivial low energy excitations of the system, and so knowledge of the core structure, topology, symmetry, dynamics and interactions of vortices reveals details of the low energy properties of the system. As well as conventional singular quantized vortices seen in ⁴He-II superfluids, one component Bose-Einstein condensates, and s-wave superconductors, there also exist more exotic quantized vortices, such as non-singular vortices, continuous vortices and composite vortices [1]. Non-singular vortices have a hard core set by the coherence length but with a non-zero order parameter within the core. Such order parameter textures have been explored in various systems, including multi-component cold atomic gases [2], nonlinear optics [3], superfluid ³He-A [1] and Sr₂RuO₄ [4]. However, the control of these structures and, in particular, their nucleation from conventional singular vortices has been elusive. In this letter we propose how these structures can be controllably created and manipulated in polariton condensates by using magnetic fields. We make use of the non-equilibrium properties of the polariton condensate, and so illustrate how a nonequilibrium condensate may show behavior not present in equilibrium spinor condensates like cold atoms or ³He-A.

Microcavity polaritons are quasiparticles that result from the hybridization of excitons and photons confined inside semiconductor microcavities. At low temperatures, they can condense, and polariton condensation has been the subject of much recent work (see [5] for a recent review). Polariton condensates differ from condensates of ultracold atomic gases or helium in that polariton condensates can be non-equilibrium systems: the photon component decays, and so new polaritons must be injected into the system to maintain a steady state. Hence, polariton condensates can be thought of as sustained nonequilibrium systems with nontrivial spatiotemporal properties. Spatiotemporal pattern formation has been extensively studied in systems such as fluid and plasma

dynamics, reaction diffusion systems, biological structures, and neural networks. Order parameter equations describe the structure and dynamics of pattern formation in these systems, and the order parameter equation for the polariton system (and closely related nonlinear optical systems [6]) is the complex Ginzburg-Landau equation (cGLE) [7]. Polariton condensates are well suited for studying pattern formation since the source term can be made to vary in space (and time) and thereby control pattern formation. Recent experiments on polaritons have begun to explore this possibility, by studying phenomena such as quantized vortices [8], soliton propagation [9], and patterns in one-dimensional samples [10].

As polaritons have a polarization degree of freedom, they can support unconventional quantized vortices, such as non-singular vortices where only one polarization component has vortices [11]. Such polariton “half-vortices” have been seen in experiments [12], but there are questions about the conditions required for them to remain stable and independent [13]. Experimental investigation of their stability is hard because observations of polariton vortices have generally relied on disorder to pin vortices [8, 12], and half-vortices could be stabilized by disorder induced strain splitting of polarization states. Theoretical alternatives to these disorder-localized vortices have been proposed, such as rotating lattices in harmonically trapped incoherently pumped condensates [14]. Direct observation of such rotating vortex lattices is however hard with current approaches to observing vortices [15, 16]. There are also proposals to create half vortices using parametric [17, 18] or coherent pumping [19]. None of these schemes combine the necessary features to experimentally investigate the stability of half vortices in a clean incoherently pumped system. This is the task we address in this letter, by showing how interplay between the synchronization-desynchronization transition of the homogeneous system [20, 21] and interference between polaritons originating from separate incoherent pumping spots can produce non-rotating lattices of vortices, where a transition between separate and locked half-vortices can be controlled by an applied magnetic field.

We start by introducing the cGLE for a spinor polariton condensate. This includes a term describing pumping, and for stability this must be nonlinear, so that it saturates as the condensate density increases. In a single component condensate, the simplest such nonlinearity is to write, $i\hbar\partial_t\psi \sim i(\gamma - \Gamma|\psi|^2)\psi$. However, as discussed recently [22], adding an energy dependent gain term $i\hbar\partial_t\psi \sim i(\gamma - \Gamma|\psi|^2 - i\eta\hbar\partial_t)\psi$ can be important to correctly describe pattern formation where energy relaxation plays an important rôle. The (dimensionless) parameter η is the rate at which gain decreases with increasing energy. In the spinor case, a further possibility emerges: there can be a cross-polarization term whereby the gain of one component may be affected by the density of the other component. These various nonlinearities can all be understood in terms of transfer between an excitonic reservoir and the condensate, driven by the lack of chemical equilibrium [23]. Nonlinearity arises both from depletion of the reservoir, and from shifts of the condensate chemical potential. We have therefore included all three types of possible nonlinearity, and studied how they affect the behavior. The spinor cGLE is thus:

$$i\hbar\partial_t\psi_{\pm} = [\pm\Omega_{\perp} - \frac{\hbar^2\nabla^2}{2m} + U_0|\psi_{\pm}|^2 + (U_0 - 2U_1)|\psi_{\mp}|^2 + iP(r, \psi_{\pm}) - i\kappa]\psi_{\pm} + \Omega_{\parallel}\psi_{\mp}, \quad (1)$$

where \pm stand for left- and right- polarizations. We first discuss the parameters describing energetics, and then turn to those related to the pump configuration and loss.

Since the nonlinear terms can be rescaled by a change of density, the only important parameter for the interactions is the ratio U_1/U_0 which we take as $U_1/U_0 = 0.55$ (see e.g. [21]). This implies a weak attraction between opposite polarizations of polaritons. The parameter Ω_{\perp} represents a magnetic field perpendicular to the 2D polariton condensate, while Ω_{\parallel} represents either an in-plane field, or the intrinsic splitting of linear polarizations present in most microcavity samples. We consider values based on the recent experiment in GaAs[24], for which a range $0 < \Omega_{\perp} < 50\mu\text{eV}$ was achieved, resulting in a transition from linear to circular polarization. The splitting Ω_{\parallel} was only constrained to be less than the linewidth. We choose a value $\Omega_{\parallel} = 3\mu\text{eV}$ consistent with this, which, as discussed below, reproduces results for the homogeneous system that may be compared to experiment. Finally, the polariton mass only controls the overall length scale $\ell_0 = \sqrt{\hbar^2/2m\kappa}$; where necessary we give lengths in terms of this scale which would be $\ell_0 = 1.95\mu\text{m}$ for $m = 10^{-4}m_e$, taking decay rate $\kappa = 0.1\text{meV}$.

We propose to form vortex lattices by pumping in three localized spots equidistant from each other. This means that the pump term $P(r, \psi_{\pm})$ is taken to be zero outside the pump spots. Inside each pump spot, including the nonlinearities discussed above, it has the form $P(r, \psi_{\pm}) = \gamma - \eta i\hbar\partial_t - \Gamma_s|\psi_{\pm}|^2 - \Gamma_x|\psi_{\mp}|^2$. We consider

pumping at 2.5 times threshold, i.e. $\gamma = 2.5\kappa$. The parameter η is not well constrained, so we consider a range of values. For the other nonlinearities, we take $\Gamma_s/U_0 = 0.3, \Gamma_x/U_0 = 0.1$, based on values discussed in [21]. The term Γ_x , describing a cross-spin nonlinearity is new, and we do not have an independent estimate of its value. However, as long as $\Gamma_x < \Gamma_s$, we find that the effect of increasing Γ_x/Γ_s is similar to the effect of increasing η . If $\Gamma_x = \Gamma_s$, the pumping process becomes spin-blind, and so the polarization state is fixed purely by the energetics.

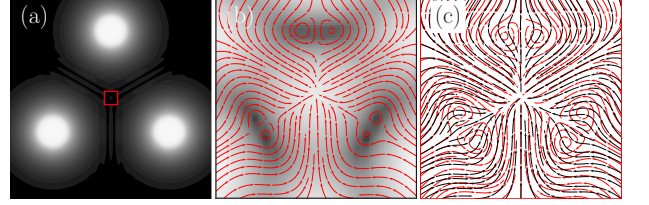


FIG. 1. Vortex lattices due to polariton flow from three pumping spots. Panel (a) shows a $40\ell_0 \times 40\ell_0$ region, illustrating the location of the pumping spots and a smaller $2\ell_0 \times 2\ell_0$ region marked by a (red) square. Panel (b) shows the streamlines and density profile of the majority component at $\Omega_{\perp} = 2.4\mu\text{eV}$ in the synchronized regime. (The minority streamlines are locked and thus equivalent). Panel (c) Show the streamlines for both polarizations (Red (gray)– majority, Black – minority) in the desynchronized regimes for $\Omega_{\perp} = 100\mu\text{eV}$. All figures are for $\gamma = 2.5\kappa, \Omega_{\parallel} = 3\mu\text{eV}, \eta = 0.1$.

If the pumping spots are irregularly spaced, then the generated currents interfere and form vortex pairs which may lead to turbulent state of interacting vortices as was discussed in [25]. However if the spots are placed sufficiently symmetrically then stationary vortex lattices form. We performed series of numerical experiments pumping at three spots of radius $R = 5\ell_0$ centered at $(0, 20)\ell_0, (\pm 10\sqrt{3}, 10)\ell_0$ (see Fig. 1). The numerical integration of Eq. (1) was done by the fourth order finite differences in space and the fourth order Runge-Kutta in time. Vortex lattices form as long as the flux leaving one spot is enough to reach the adjacent spots, and thus cause synchronization; this is very similar to what was found for polariton condensates trapped in disorder potentials [20], however here we have no trapping potential. Vortex lattices are thus visible only for large enough γ/κ and small enough η . Fig. 1 is for parameters where synchronization between spots just occurs, and as a result, the lattice is not perfectly hexagonal; for larger α , lattices are more hexagonal (not shown). Synchronization of pump spots, and the consequent vortex lattices, can also survive some degree of imperfection in size and location, 10% variations can be tolerated for the parameters used in Fig. 1.

For conditions where a vortex lattice occurs, we then vary the detuning Ω_{\perp} and observe the evolution of vortex lattices. As Ω_{\perp} increases, there is a transition from an

elliptically polarized condensate to a state where the two circular polarization components desynchronize, producing two separate condensates, with two separate chemical potentials (frequencies). In the synchronized regime, integer vortex lattices are formed with vortices of the same circulation of the two polarizations sitting on the top of each other. In the desynchronized regime, the lattice of the majority component survives, but a number of possible behaviors for the minority component can occur, depending on the values of $\gamma/\kappa, \eta, \Omega_\perp$. In Fig. 1(c), the minority component has a vortex-free state. There can also be cases where a vortex lattice survives for the minority component, but because the polarization components are not synchronized, the position of these minority vortices can oscillate in time. For large γ/κ , these oscillations are small, and only a slight shift of the minority lattice is visible. However, for $\gamma = 2.5\kappa$ as shown in Fig. 1(c), there is a clear transition to a half-vortex lattice. At much larger Ω_\perp , a transition back to a synchronized state is seen, but for $\eta = 0.1$, this is far beyond the range of Ω_\perp achievable in experiment.

Having illustrated how the desynchronization transition has dramatic effects on the vortex lattices, we derive analytic approximations for the period of the vortex lattice, and the critical field for the desynchronization transition, by using a generalized local-density approximation (considering also the phase gradients), and making use of results for a homogeneously pumped system. The period of the vortex lattice can be understood by finding the wavelength of the phase variation at points far from a pump spot. If the pump spot is large then currents can be neglected within the pump spot, and the homogeneous system used to predict whether the system is synchronized, and the values of chemical potential. When synchronized, $i\partial_t\psi_\pm = \mu\psi_\pm$, and so Eq. (1) becomes a pair of time-independent differential equations. To solve these, it is convenient to write $\psi_\pm = \sqrt{\rho_\pm}e^{i(\phi_\pm\theta/2)}$. In the synchronized case θ is constant so the lattice spacing is set by the velocity $\mathbf{u} = \hbar\nabla\phi/m$. Far away from the pump spot, the pump term vanishes, and the density decays and so interaction terms $U\rho_\pm$ can be neglected. With these approximations the real and imaginary parts of Eq. (1) become: $\mu - \frac{1}{2}m|\mathbf{u}|^2 \mp \Omega_\perp = \Omega_\parallel\sqrt{\rho_\pm/\rho_\mp}\cos(\theta)$ and $\frac{1}{2}\hbar\nabla \cdot (\rho_\pm\mathbf{u}) = -\kappa\rho_\pm \pm \Omega_\parallel\sqrt{\rho_+\rho_-}\sin(\theta)$. These equations are solved by $\sin(\theta) = 0, \rho_+ \propto \rho_-$ and thus $\frac{1}{2}m|\mathbf{u}|^2 = \mu + (\Omega_\parallel^2 + \Omega_\perp^2)^{1/2}$. When desynchronized, a general solution is more complicated, as θ and ρ_+/ρ_- are time dependent, and one must find the average $\langle|\mathbf{u}_\pm|^2\rangle$ in terms of $\langle\mu_\pm\rangle$. However, if $\rho_- \gg \rho_+$ in the desynchronized region, then the real part of Eq. (1) for the majority component becomes $\frac{1}{2}m\langle|\mathbf{u}_-|^2\rangle = \langle\mu_- \rangle + \Omega_\perp$. The hexagonal vortex lattice resulting from the interference of three such currents has a spacing $l = (2/3\sqrt{3})(\hbar/m|\mathbf{u}|)$. For the parameters of Fig. 1, this gives $l = 1.4\ell_0$, consistent with the observed lattice. For larger $\Omega_\perp, \Omega_\parallel$, the

lattice spacing is found to vary considerably with Ω_\perp ; we have checked that the form discussed here matches the numerical simulations well.

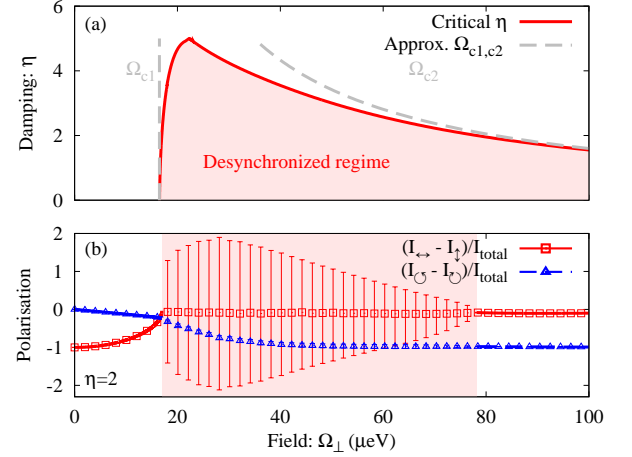


FIG. 2. Panel (a): boundary of desynchronized region as a function of field Ω_\perp and relaxation rate η for homogeneous pumping. Solid lines are exact numerical results; gray dashed lines are the approximate asymptotes given in the text. Panel (b): polarization degree vs. field Ω_\perp for the homogeneous system at $\eta = 2$. Lines indicate the steady state polarization for the synchronized regimes. The points and error bars indicate the time-average, and envelope of polarization oscillations. (NB the envelopes are normalized by the average, rather than instantaneous, intensity.)

We next discuss the critical fields required to switch between synchronized and desynchronized lattices, as shown in Fig. 2(a). The line in Fig. 2 is calculated for homogeneous pumping; numerical simulations with inhomogeneous pumping also respect this boundary, i.e. the critical Ω_\perp for desynchronization is rather robust to inhomogeneity. Analytical estimates of the critical fields $\Omega_\perp, \Omega_\parallel$ help to reveal how they depend on the system parameters. The first transition on increasing Ω_\perp is from the elliptically polarized (synchronized) phase existing for small Ω_\perp to a desynchronized state. This transition was discussed in Refs. [20, 21]. If $\Omega_\perp, \Omega_\parallel \ll 2U_1(\rho_+ + \rho_-)$ (which is the case for the current parameters), then one may approximate the coupled equations for θ, ρ_\pm (with the parametrization $\psi_\pm = \sqrt{\rho_\pm}e^{i(\phi_\pm\theta/2)}$ introduced above) by using standard results for Josephson oscillations in the Josephson regime [26]. The transition thus occurs at $\Omega_\perp = \Omega_{c1} \simeq 2U_1\Omega_\parallel/(\Gamma_s - \Gamma_x)$.

If $\eta \neq 0$ there is another transition at $\Omega_\perp = \Omega_{c2}$ back to a synchronized state. The critical field Ω_{c2} can be estimated analytically by linear stability analysis of the synchronized state at $\Omega_\perp > \Omega_{c2}$. Since $\rho_- \gg \rho_+$ in this large Ω_\perp limit, one may show that fluctuations of $\rho_+ - \rho_-$ relax quickly. The remaining part of the linearized

Eq. (1) can be written in terms of $\zeta = \psi_+^* \psi_-$ as:

$$(1 + \eta^2) \hbar \partial_t \zeta = (\gamma_{\text{eff}} - i\nu_{\text{eff}}) \zeta - \Omega_{\parallel} \rho_- (\eta + i). \quad (2)$$

where $\gamma_{\text{eff}} = 2(\gamma - \kappa) - \rho_- [\Gamma_s + \Gamma_x + 2\eta(U_0 - U_1)]$ and $\nu_{\text{eff}} = 2\Omega_{\perp} + [\eta(\Gamma_s - \Gamma_x) - 2U_1] \rho_-$. Instability of the synchronized state occurs when γ_{eff} becomes negative, thus to find Ω_{c2} one thus needs $\rho_- (\Omega_{\perp})$ at large Ω_{\perp} . Since $\rho_- \gg \rho_+$, one may simplify Eq. (1) for ψ_- considerably to give $\rho_- \simeq (\gamma - \kappa + \eta\Omega_{\perp})/(\eta U_0 + \Gamma_s)$ hence one has

$$\Omega_{c2} \simeq \frac{(\gamma - \kappa)}{\eta} \frac{\Gamma_s - \Gamma_x + 2\eta U_1}{\Gamma_s + \Gamma_x + 2\eta(U_0 - U_1)}. \quad (3)$$

As the relaxation rate η increases Ω_{c2} becomes smaller, and eventually the desynchronized regime will vanish.

Let us now briefly consider the relation of the experimental results of Larionov *et al.* [24] to the polarization desynchronization transition. In their experiment, a transition was seen such that for small Ω_{\perp} a single frequency elliptically polarized condensate was observed, and above a critical value of Ω_{\perp} , a transition to a Zeeman split condensate, with separate frequencies for left- and right-circular components was observed. While it was noted in [24] that some features of the experimental results clearly required aspects of non-equilibrium physics, the transition was interpreted as a signature of the equilibrium transition to a circular condensate [27]. However, a fragmented condensate (i.e. having multiple condensate frequencies) is not expected in equilibrium, but is precisely the signature expected for the desynchronization transition. While this identification would require further experimental corroboration, we have chosen our value of $\Omega_{\parallel} = 3\mu\text{eV}$ so the desynchronization transition matches this experimental transition. Figure 2(b) illustrates the behavior in the desynchronized regime, showing the amplitude of polarization fluctuations. The time averaged polarization degree shown in that figure evolves smoothly with field, and so provides a poor distinction between synchronized and desynchronized behavior. One may however note that both Ω_{c2} , and the equilibrium critical field [27] increase with density. In contrast, Ω_{c1} , where splitting of the condensate frequencies should occur due to desynchronization is independent of density (for small enough η). This may provide a clear way to distinguish the nature of the transition observed experimentally [24].

In conclusion, we have explored the desynchronization transition in a non-equilibrium spinor polariton condensate, and shown how this transition can be used to drive a system between lattices of integer and half vortices. Using the parameters of recent experiments [24], we show that the conditions for the desynchronization transition seem likely to be achievable, and note that aspects of the experimentally observed behavior may even suggest that the transition already seen is that to a desynchronized state, rather than to a circularly polarized state.

When the ability to control polarization via magnetic field is combined with the possibility to form static vortex lattices via symmetric pumping spots, our proposed scheme illustrates how one may engineer and control exotic lattice spin textures deterministically using incoherently pumped polariton condensates.

J.K. acknowledges funding from EPSRC grant EP/G004714/2. N.G.B acknowledges EU FP7 ITN project CLERMONT4.

-
- [1] G. E. Volovik, *The Universe in a Helium Droplet* (Oxford University Press, Oxford, 2003).
 - [2] G. Ruben, M. Morgan, and D. Paganin, *Phys. Rev. Lett.* **105**, 220402 (2010).
 - [3] L. Pismen, *Phys. Rev. Lett.* **72**, 2557 (1994).
 - [4] A. P. Mackenzie and Y. Maeno, *Rev. Mod. Phys.* **75**, 657 (2003).
 - [5] H. Deng, H. Haug, and Y. Yamamoto, *Rev. Mod. Phys.* **82**, 1489 (2010).
 - [6] K. Staliūnas and V. J. Sánchez-Morcillo, *Transverse Patterns in Nonlinear Optical Resonators*, Springer Tracts in Modern Physics, Vol. 183 (Springer-Verlag, Berlin, 2003).
 - [7] I. S. Aranson and L. Kramer, *Rev. Mod. Phys.* **74**, 99 (2002).
 - [8] K. G. Lagoudakis *et al.*, *Nature Phys.* **4**, 706 (2008).
 - [9] A. Amo *et al.*, *Nature* **457**, 291 (2009).
 - [10] E. Wertz *et al.*, *Nat. Phys.* **6**, 860 (2010).
 - [11] Y. G. Rubo, *Phys. Rev. Lett.* **99**, 106401 (2007).
 - [12] K. G. Lagoudakis *et al.*, *Science* **326**, 974 (2009).
 - [13] H. Flayac, I. A. Shelykh, D. D. Solnyshkov, and G. Malpuech, *Phys. Rev. B* **81**, 045318 (2010); M. T. Solano and Y. G. Rubo, *Phys. Rev. B* **82**, 127301 (2010).
 - [14] J. Keeling and N. G. Berloff, *Phys. Rev. Lett.* **100**, 250401 (2008).
 - [15] G. Roumpos *et al.*, *Nat. Phys.* **7**, 129 (2011).
 - [16] K. G. Lagoudakis *et al.*, *Phys. Rev. Lett.* **106**, 115301 (2011).
 - [17] A. V. Gorbach, R. Hartley, and D. V. Skryabin, *Phys. Rev. Lett.* **104**, 213903 (2010).
 - [18] S. Pigeon, I. Carusotto, and C. Ciuti, *Phys. Rev. B* **83**, 144513 (2011).
 - [19] T. C. H. Liew, Y. G. Rubo, and A. Kavokin, *Phys. Rev. Lett.* **101**, 187401 (2008).
 - [20] M. Wouters, *Phys. Rev. B* **77**, 121302 (2008).
 - [21] M. O. Borgh, J. Keeling, and N. G. Berloff, *Phys. Rev. B* **81**, 235302 (2010).
 - [22] M. Wouters and I. Carusotto, *Phys. Rev. Lett.* **105**, 020602 (2010); M. Wouters and V. Savona, arXiv:1007.5453; M. Wouters, T. C. H. Liew, and V. Savona, *Phys. Rev. B* **82**, 245315 (2010).
 - [23] A. Griffin, T. Nikuni, and E. Zaremba, *Bose-Condensed Gases at Finite Temperatures* (Cambridge University Press, Cambridge, 2009).
 - [24] A. Larionov *et al.*, *Phys. Rev. Lett.* **105**, 256401 (2010).
 - [25] N. G. Berloff, arXiv:1010.5225.
 - [26] A. J. Leggett, *Rev. Mod. Phys.* **73**, 307 (2001).
 - [27] Y. G. Rubo, A. V. Kavokin, and I. A. Shelykh, *Phys. Lett. A* **358**, 227 (2006); J. Keeling,

Phys. Rev. B **78**, 205316 (2008).